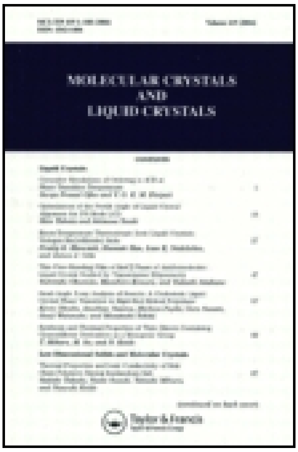


Molecular Crystals and Liquid Crystals
Publication details, including instructions for authors and subscription information:
http://www.tandfonline.com/loi/gmcl20

# Coplanar Liquid Crystal Reconfigurable Phase-Shifters

F. Sahbani [a b c d e], N. Tentillier [a b c d], C. Legrand [a b c d], K. Blary [a e f], A. Gharsallah [g] & A. Gharbi [g]

[a] Univ Lille Nord de France, Lille, France
[b] ULCO, UDSMM, Calais, France
[c] USTL, UDSMM, Calais, France
[d] CNRS, EAC, Calais, France
[e] USTL, IEMN, Villeneuve d'Ascq, France
[f] CNRS, UMR, Villeneuve d'Ascq, France
[g] Faculté des Sciences de Tunis, LPMM, Tunis, Tunisia

Version of record first published: 14 Jun 2011

To cite this article: F. Sahbani, N. Tentillier, C. Legrand, K. Blary, A. Gharsallah & A. Gharbi (2011): Coplanar Liquid Crystal Reconfigurable Phase-Shifters, Molecular Crystals and Liquid Crystals, 542:1, 204/[726]-212/[734]

To link to this article: http://dx.doi.org/10.1080/15421406.2011.570587

*Mol. Cryst. Liq. Cryst.*, Vol. 542: pp. 204/[726]–212/[734], 2011

ISSN: 1542-1406 print/1563-5287 online
DOI: 10.1080/15421406.2011.570587



# Coplanar Liquid Crystal Reconfigurable Phase-Shifters

F. SAHBANI,[1,2,3,4,5] N. TENTILLIER,[1,2,3,4] C. LEGRAND,[1,2,3,4] K. BLARY,[1,5,6] A. GHARSALLAH,[7] AND A. GHARBI[7]

[1]Univ Lille Nord de France, Lille, France
[2]ULCO, UDSMM, Calais, France
[3]USTL, UDSMM, Calais, France
[4]CNRS, EAC, Calais, France
[5]USTL, IEMN, Villeneuve d'Ascq, France
[6]CNRS, UMR, Villeneuve d'Ascq, France
[7]Faculté des Sciences de Tunis, LPMM, Tunis, Tunisia

*A coplanar liquid crystal phase-shifter is presented and characterized in the frequency range of 5–40 GHz. The interest of this structure lies in the technological realization which is very simple. The phase-shift variation is of 0.2°/cm/GHz for an attenuation of 2.5 dB/cm at 40 GHz. These performances are in agreement with those predicted in a preliminary theoretical study.*

**Keywords** Coplanar LC phase-shifter; liquid crystal; micro-strip; microwave devices

## 1. Introduction

Frequency tunable devices are circuits whose frequency response can be modified with an external drive. Such devices present applications in telecommunications. For example, tunable phase-shifters can be used as element of electronic scanning antennas.

In the last decade, liquid crystals (LC) have been investigated as active dielectric for tunable microwave devices [1–6]. This represents a new application of these materials largely used in visualization displays. Liquid crystals were used to realize tunable phase-shifters, planar antennas and filters [7–14]. LC present good potentialities among them, low driving electric field (typical 0.2 V/μm) and relatively low dielectric losses at millimeter wavelength. However, the decrease in switching times (especially the switching off time) still represents a challenge even if some solutions are possible: low thickness active layer dual frequency driving, ferroelectric liquid crystals [15–17]. Typically, LC birefringence value is about 0.1 and the maximum phase-shift variation of tunable LC phase-shifters is lower than 1°/cm/GHz.

Address correspondence to F. Sahbani, Univ Lille Nord de France, F-59000 Lille, France. Tel.: +33617040918; Fax: +33321465778; E-mail: sahbanifehim@yahoo.fr

Most LC tunable phase-shifters are based on microstrip structures [18–21]. Here, we are interested in coplanar LC tunable phase-shifters. To our knowledge, such a study on coplanar LC phase-shifters without floating electrode [8] was not reported in the literature.

The device principle is first described in the next section. Then, we give the results of microwave dielectric characterization of the liquid crystal. This dielectric data is used to perform a preliminary theoretical study. Finally, a coplanar phase-shifter is realized and the experimental results and performances are given.

## 2. Coplanar Phase-Shifters Principle

The structure of the coplanar phase-shifter is given in Figures 1 and 2. The access lines and the active part are made of coplanar lines so that coplanar type propagation is maintained in all the structure. To improve liquid crystal orientation, an isolating substrate is placed on the active part in which the liquid crystal is introduced by capillarity. The characteristic impedance of the access lines is 50 Ω. The characteristic impedance of the active part is maintained at 50 Ω in changing the strip width (W) and the gap (G) without changing the ground planes distance (W + 2 G).

The basic principle to explain tunability is given in Figure 3. An initial ($V_{AC} = 0$ V) planar molecular orientation with a main alignment direction along the propagation axis is fixed by surface treatment (polymer layer coating and rubbing). Under a low frequency driving electric field $E_{AC}$, the molecules reorient due to the coupling with the low frequency dielectric positive anisotropy (rotation axis perpendicular to the electrodes). At high electric field, the molecules are perpendicular to the propagation direction.

Therefore, the radio-frequency active permittivity goes continuously from $\varepsilon_\perp$ to $\varepsilon_\parallel$. These permittivities correspond respectively to the case of an electric field $E_{RF}$ perpendicular or parallel with the director n. For a matched line, the phase-shift variation for a driving voltage V is:

$$\Delta\varphi(V) = \frac{2\pi f\ L\ \Delta n_{eff}(V)}{c} \quad \text{with} \quad \Delta n_{eff}(V) = \sqrt{\varepsilon_{eff}(V)} - \sqrt{\varepsilon_{eff\perp}} \qquad (1)$$

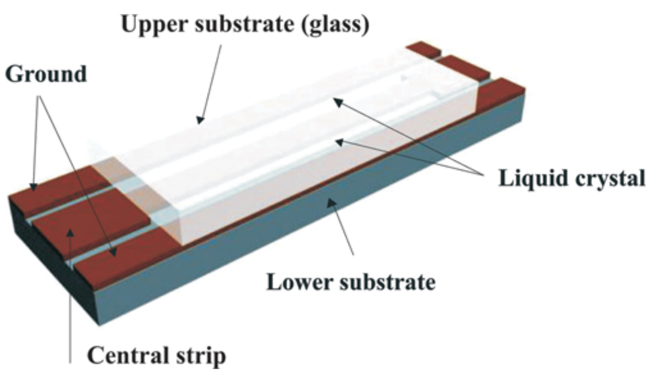


**Figure 1.** Overview of the coplanar phase-shifter. (Figure appears in color online.)

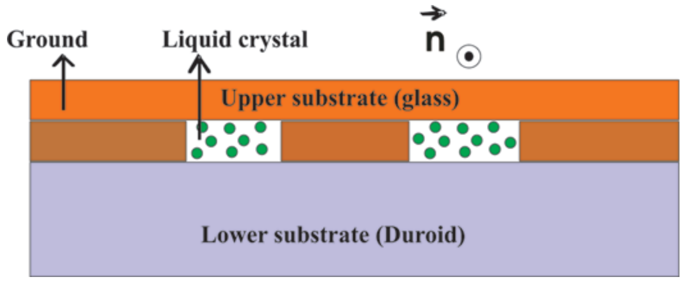


**Figure 2.** Cross-section view of the coplanar phase-shifter. (Figure appears in color online.)

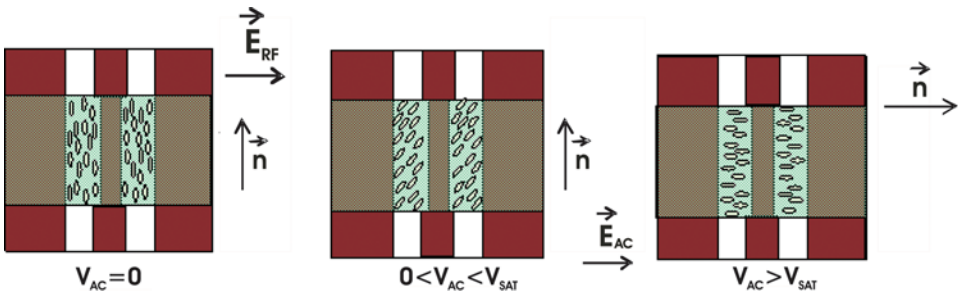


**Figure 3.** Coplanar phase-shifter principle. (Figure appears in color online.)

where f is the frequency, c the vacuum velocity, L the line length and $\Delta n_{eff}(V)$ is the effective birefringence. The maximum phase-shift variation is obtained at high driving voltage assuming $\varepsilon'_{eff}(V) = \varepsilon'_{eff\parallel}$:

$$\Delta\varphi_{\max} = \frac{2\pi f L \Delta n_{eff}}{c} \quad \text{with} \quad \Delta n_{eff} = \sqrt{\varepsilon_{eff\parallel}} - \sqrt{\varepsilon_{eff\perp}} \tag{2}$$

In practice, gap G is reduced (typically $<100\,\mu m$) to decrease the driving voltage (driving electric field $E = V/G$). The liquid crystal thickness and therefore the response times are directly connected with the conductive strips thickness.

A part of the electric field lines are in the insulating substrates. Then, for a given liquid crystal, tunability should be lower for a coplanar phase-shifter than for micro-strip ones. However, the realization technology of these phase-shifters is very simple and this represents their interest.

## 3. Dielectric Characterization of the Nematic Liquid Crystal

We performed microwave dielectric characterization using the rectangular wave-guide techniques in the frequency range 26–40 GHz (Ka band 7.1 mm × 3.56 mm). Measurements were performed with a vectorial network analyzer (Anritsu 37369A). The empty cell and the filled cell are measured successively without disassembly and without calibration of the vectorial network analyser. The measurement

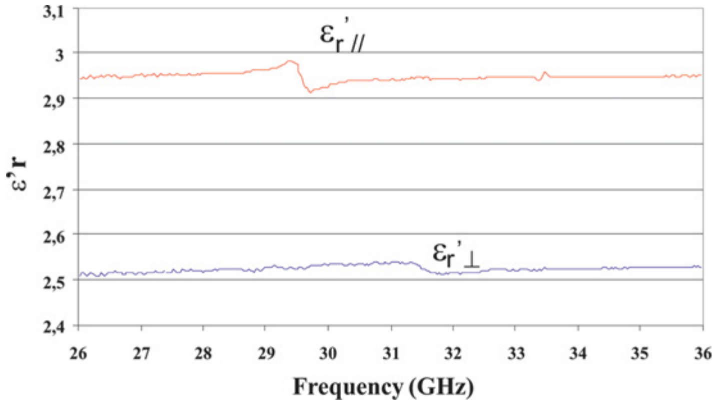


**Figure 4.** Real permittivity of 5CB versus frequency. (Figure appears in color online.)

data are then treated using a specific method to determine the complex permittivity of the sample [22]. The director of the LC is orientated in applying an external high magnetic field (≈1 Tesla).

The classical commercial liquid crystal (K15 Merck) namely, 4-pentyl-4′-cyano-biphenyl is used in this study. This liquid crystal exhibits a nematic phase at room temperature (22–35°C). The experimental results for the real permittivity and the loss factor ($tg\delta = \varepsilon''/\varepsilon'$) are given in Figures 4 and 5. The peaks at 29–30 GHz and 31–32 GHz are connected to measurement errors and do not exist.

As expected, the real permittivities are frequency independent and the dielectric losses are low. The dielectric data are the following: $\varepsilon'_{\parallel 5CB} = 2.98$, $\varepsilon'_{\perp 5CB} = 2.64$, $\varepsilon''_{\parallel 5CB} = 0.04$, $\varepsilon''_{\perp 5CB} = 0.08$. The microwave birefringence is found to be: $\Delta n_{5CB} = \sqrt{2.98} - \sqrt{2.64} = 0.1$. Such an effective birefringence would correspond to a phase-shift variation of 1.2°/cm/GHz (Eq. (2)). Dielectric data are used in the next section to perform a preliminary theoretical study of coplanar phase-shifters.

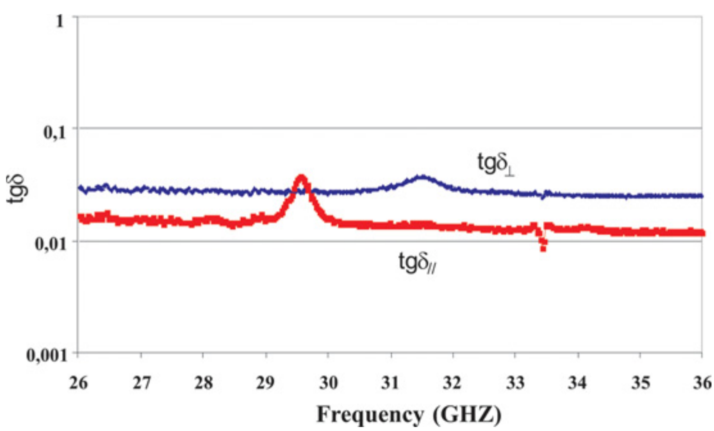


**Figure 5.** Losses factor of 5CB versus frequency.

## 4. Preliminary Theoretical Study

For this study, we used an analytical model developed for coplanar lines [23]. We have adapted this model to the structure of the active part (Fig. 2), taking into account the permittivity of the top substrate (different of unity) and the conductive strip line thickness. The model calculates the equivalent capacities of each part of the device, the effective permittivity and the characteristic impedance.

In Figure 6, we give the evolution of the central strip width W versus the gap G to maintain a characteristic impedance of 50 Ω as a function of the conductive strips thickness t. The lower and upper substrates are respectively made of Duroid 4003 Rogers ($\varepsilon' = 3.38$, h = 508 μm) and glass ($\varepsilon' = 5$, h = 700 μm).

At a given gap G, the central strip width decreases with the conductive strip thickness. At high gaps (G > 60 μm), the ratio W/G is about 3. At lower gaps, this ratio strongly decreases.

The analytic model is also used to predict the tunability of coplanar phase-shifters. For this, at a given gap G, the central strip W is first fixed to obtain a characteristic impedance of 50 Ω for $\varepsilon'_{CL} = \varepsilon'_{\perp 5CB} = 2.63$. Then, the effective permittivities $\boldsymbol{\varepsilon}'_{\mathbf{eff}\perp}$ and $\boldsymbol{\varepsilon}'_{\mathbf{eff}\parallel}$ and the effective birefringence $\Delta n_{eff} = \sqrt{\varepsilon'_{eff\parallel}} - \sqrt{\varepsilon'_{eff\perp}}$ are determined. These permittivities correspond to the case of an active permittivity of the liquid crystal equal to $\boldsymbol{\varepsilon}'_{\perp\mathbf{5CB}}$ and $\varepsilon'_{\parallel\mathbf{5CB}}$ respectively. The tunability T compare the effective birefringence $\Delta n_{eff}$ of the device with the birefringence of the liquid crystal $\Delta n_{CL}$:

$$T\ (\%) = 100\frac{\Delta n_{eff}}{\Delta n_{CL}} \tag{3}$$

The tunability T versus the gap G is reported in Figure 7.

The tunability is strongly related to the conductive strips thickness and the gap: a high conductive strip thickness and a low gap increase the tunability. As expected, the tunability of a coplanar phase-shifter should be lower than that of a microstrip

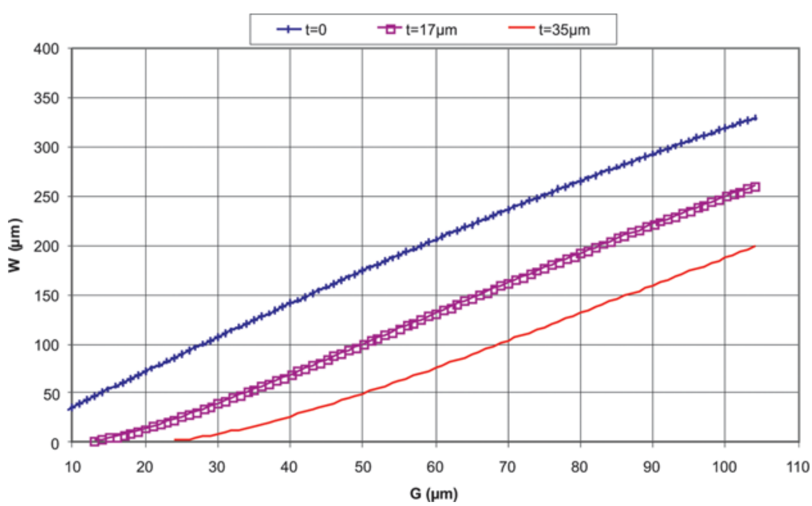


**Figure 6.** Central strip width W versus the gap G: Zc = 50Ω, $\varepsilon'_{CL} = \varepsilon'_{\perp 5CB} = 2.63$.

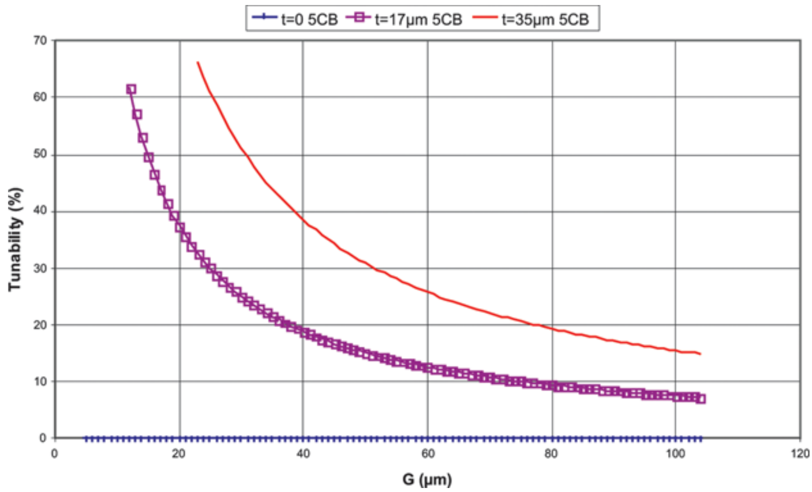


**Figure 7.** Evolution of the tunability of the coplanar phase-shifter versus the gap G.

phase-shifter (T > 70%). This is explained by the fact that only a part of the electric field lines are in the liquid crystal. The part of the electric field lines in the substrates does not contribute to the tunability (fixed permittivities). For example, a tunability of 38% corresponds to a maximum phase shift variation of 0.45°/cm/GHz for 5CB liquid crystal.

## 5. Experimental Results

Scattering matrix measurements are performed in the frequency range (5–40 GHz) using a vectorial network analyser (Anritsu 37369A). Contacts are taken with coplanar microwave probes (Picoprobe, maximum width of 440 µm) with micrometric displacements and optical checking. A Short-Open-Load-Thru calibration is carried out using calibration substrate (CS-5). The access lines are taken into account to obtain the phase-shifter characteristics. The driving electric field (sinusoidal, f = 10 kHz) is applied via network analyzer external bias.

The lower substrate is realized by photolithography and chemical etching on presensibilized and coppered substrates. The dimensions of the phase shifter's active part are the following: G = 40 µm, W = 100 µm, t = 35 µm and L = 14 mm. The liquid crystal is introduced by capillarity filling after a surface treatment (PVA coating and rubbing).

The amplitude of the reflexion and transmission coefficients versus frequency is given in Figures 8 and 9. Without driving, a good matching of the device is observed ($|S_{11}| < -15$ dB).

The attenuation ($|S_{12}|$) is limited to 3.7 dB at 40 GHz (2.5 dB/cm). At high driving voltage, the amplitude of $S_{11}$ parameter increases ($< -6$ dB at 40 GHz). This can be understood from the CL permittivity variation.

The $S_{12}$ phase and the $S_{12}$ phase variation as a function of frequency are given in Figures 10 and 11. The $S_{12}$ phase variation is calculated from the difference between the $S_{12}$ phase measured with and without driving voltage (0 V and 10 V). The $S_{12}$ phase evolves linearily with frequency. At 40 GHz, the value of the phase variation is 11.5°.

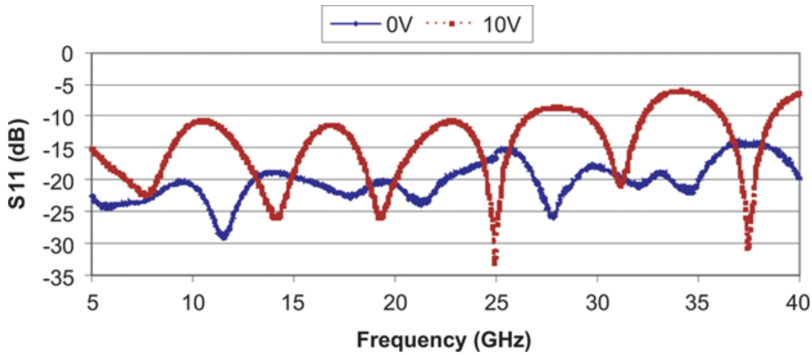


**Figure 8.** Reflexion coefficient modulus $|S_{11}|$ versus frequency.

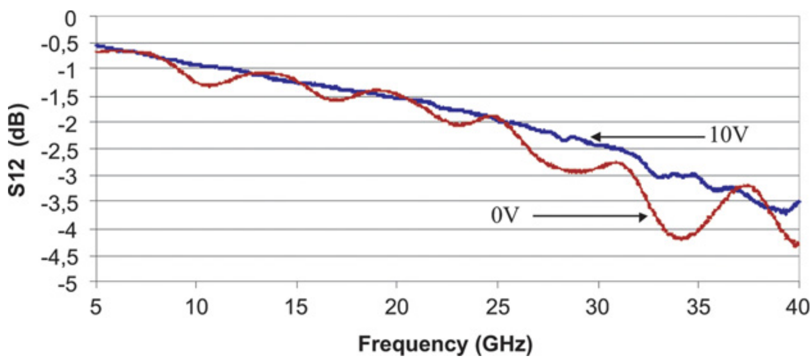


**Figure 9.** Transmission coefficient modulus $|S_{12}|$ versus frequency.

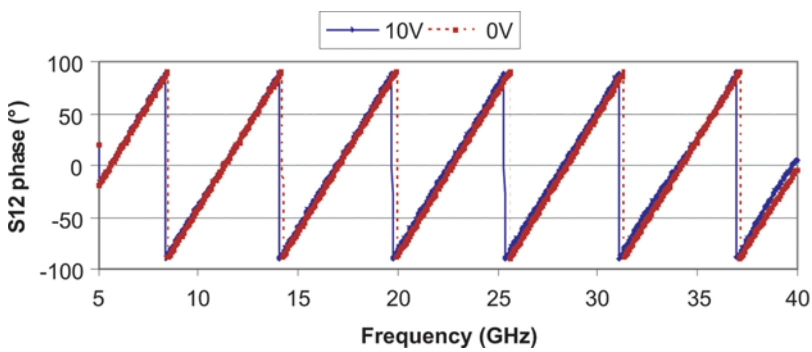


**Figure 10.** $S_{12}$ phase versus frequency (bias 0 V__, 10 V__).

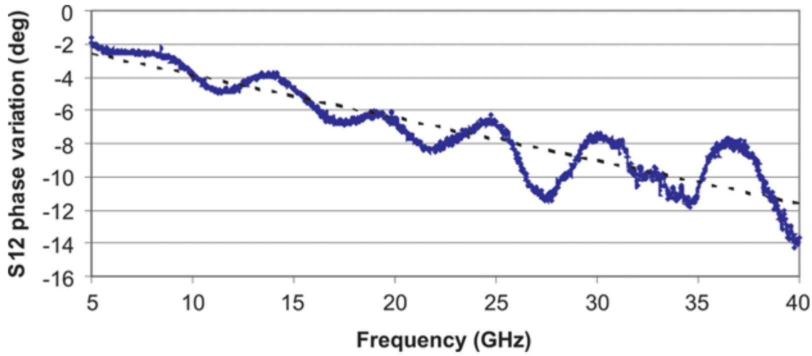


**Figure 11.** $S_{12}$ phase variation versus frequency.

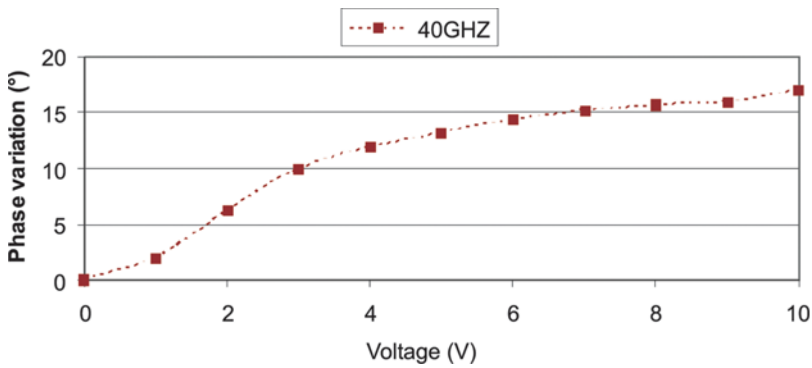


**Figure 12.** $S_{12}$ phase variation versus driving voltage (40 GHz). (Figure appears in color online.)

This corresponds to 0.2°/cm/GHz and to a tunability of 17%. This value is lower than theoretical predictions (Fig. 7) and could be improved. In Figure 12, we give the $S_{12}$ phase variation evolution versus driving voltage. Saturation phenomenon occurs at about 7 V (E = 0.17 V/µm).

## 6. Conclusions and Perspectives

This study focuses on the realization and the characterization of a coplanar LC phase-shifter. These phase-shifters offer simple technological realization whereas the tunability is lower than that of microstrip structures. A possibility of improving the tunability woud be to increase the sample thickness. Studies on switching times and use of a large birefringence LC are also in progress.

## Acknowledgment

The authors would like to express their thanks to the Plateforme Technologique "Simulation et Prototypage de Cartes Electroniques" especially N. Verbrugghe and K. Binet for the neat realization of circuits.

## References

[1] Guerin, F., Chappe, J.-M., Joffre, P., & Dolfi, D. (1997). *Japanese Journal of Applied Physics*, *36*(7A), 4409–4413.
[2] Splingart, B., Tentillier, N., Huret, F., & Legrand, C. (2000). *Mol. Cryst. and Liq. Cryst.*, *368*, 183–190.
[3] Weil, C., Luessem, G., & Jakoby, R. (2002). *IEEE MTT-S International Microwave Symposium Digest*, *1*, 367–370.
[4] Mueller, S., Felber, C., Scheele, P., Wittek, M., Hock, C., & Jakoby, R. (2005). *European Microwave Conference*, Paris.
[5] Toshiaki, N., Susimu, Y., Yukiko, S., Ryota, I., & Michinori, H. (2008). *Japanese Journal of Applied Physics*, *47*(11), 8483–8486.
[6] Goelden, F., Gaebler, A., Goebel, M., Manabe, A., Mueller, S., & Jakoby, R. (2009). *Electron. Lett.*, *45*(13), 686–687.
[7] Goelden, F., Gaebler, A., Mueller, S., Lapanik, A., Haase, W., & Jakoby, R. (2008). *Electronics Letters*, *44*(7), 480–481.
[8] Utsumi, Y., Bach, N. T., Kamei, T., Ozaki, R., & Moritake, H. (2009). *Mol. Cryst. and Liq. Cryst.*, *510*, 197–213.
[9] Martin, N., Prigent, G., Laurent, P., Gelin, P. H., & Huret, F. (2004). *Microwave and Optical Technology Letters*, *43*(4), 338–341.
[10] Weil, C., Müller, St., Scheele, P., Best, P., Lüssem, G., & Jakoby, R. (2003). *Electron. Lett.*, *39*(24), 1732–1734.
[11] Dubois, F., Krasinski, F., Splingart, B., Tentillier, N., Legrand, C., Spadlo, A., & Dabrowski, R. (2008). *Japanese Journal of Applied Physics*, *47*(5), 3564–3567.
[12] Popov, M. A., Zavislyak, I. V., & Srinivasan, G. (2010). *Electronics Letters*, *46*(8), 569–570.
[13] Zheng, S. Y., Chan, W. S., & Man, K. F. (September, 2010). *Microwave and Wireless Components Letters*, *20*(9), 498–500.
[14] Bulja, S., & Mirshekar-Syahkal, D. (May 2010). *Electronics Letters*, *46*(11), 27, 769–771.
[15] Palego, C., Peng, Z., Hwang, J. C. M., Scarbrough, D., & Goldsmith, C. L. (2010). *IEEE 11th Annual Wireless and Microwave Technology Conference,* WAMICON 2010, Article number 5461851.
[16] Tang, H., Yang, C., Zhang, J., Chen, H., Yu, A., He, W., & Liao, Y. (July 2010). *Journal of Infrared, Millimeter, and Terahertz Waves*, *31*(7), 852–857.
[17] Zhang, J., Zhao, J., Li, R., Peng, R., Zhang, R. J., & Wang, M. (2010). *Japanese Journal of Applied Physics*, *49*(3), PART 1.
[18] Zheng, Y., & Saavedra, C. E. (2010). *IEEE Transactions on Circuits and Systems I: Regular Papers*, *57*(4), 752–758.
[19] Nozokido, T., Maede, S., Miyasaka, N., Okada, H., Nose, T., & Murai, T. (25 January 2010). *IEICE Electronics Express*, *7*(2), 67–72.
[20] Lambard, T., Lafond, O., Himdi, M., Jeuland, H., & Bolioli, S. (February 2010). *Microwave and Optical Technology Letters*, *52*(2), 283–285.
[21] Tang, X., & Mouthaan, K. (2007). *IEEE Conference on Electron Devices and Solid-State Circuits 2007,* EDSSC 2007, 997–1000.
[22] Tentillier, N. (2003). *PhD Université du Littoral Côte d'Opale, N° 3400 December*.
[23] Gupta, K. C. (1996). *Microstrip Lines and Slotlines,* 2nd Ed., Artech House Publishers: UK.